

Neutron-capture elements in the metal-poor globular cluster M15¹

Kaori Otsuki

University of Chicago, Chicago, IL 60637, USA

otsuki@oddjob.uchicago.edu

Satoshi Honda, Wako Aoki, Toshitaka Kajino

National Astronomical Observatory, Mitaka, Tokyo 181-8588 JAPAN

aoki.wako@nao.ac.jp, honda@optik.mtk.nao.ac.jp, kajino@nao.ac.jp

and

Grant J. Mathews

University of Notre Dame, Notre Dame, IN 46556, USA

gmathews@nd.edu

ABSTRACT

We report on observations of six giants in the globular cluster M15 (NGC 7078) using the Subaru Telescope to measure neutron-capture elemental abundances. Our abundance analyses based on high-quality blue spectra confirm the star-to-star scatter in the abundances of heavy neutron-capture elements (e.g., Eu), and no significant s-process contribution to them, as was found in previous studies. We have found, for the first time, that there are anti-correlations between the abundance ratios of light to heavy neutron-capture elements ([Y/Eu] and [Zr/Eu]) and heavy ones (e.g., Eu). This indicates that light neutron-capture elements in these stars cannot be explained by only a single r-process. Another process that has significantly contributed to the light neutron-capture elements is required to have occurred in M15. Our results suggest a complicated enrichment history for M15 and its progenitor.

Subject headings: globular clusters: individual(M15) — nuclear reactions, nucleosynthesis, abundances — stars: abundances

¹Based on data collected at the Subaru Telescope, which is operated by the National Astronomical Observatory of Japan.

1. Introduction

The $[\text{Fe}/\text{H}]$ ratio for stars within a globular cluster are generally nearly identical to within $\sim 10\%$ with a few exceptions (e.g., ω - Cen and M22) ². Thus, stars within a cluster are thought to have been formed from material having an almost homogeneous chemical composition. Furthermore, once globular clusters form, their stars could not have been enriched by subsequent epochs of explosive events and star formation. Since the r-process elements observed to be present in globular clusters could only have been formed by explosive events, their abundance distributions provide a fossil record of the early Galaxy enrichment epoch just prior to the formation of globular clusters.

However, Sneden et al. (1997) have reported a significant spread in $[\text{Ba}/\text{Fe}]$ and $[\text{Eu}/\text{Fe}]$ based on observations of 18 giants in M15, suggesting a bimodal distribution of these abundances. Sneden et al. (2000a) extended the study to 31 stars in M15, although only the Ba abundances were reported due to the narrower wavelength coverage. That study confirmed the scatter of Ba abundances in stars of M15. Sneden et al. (2000b) reported on the abundance patterns of neutron-capture elements of three red giants in M15 based on high-resolution blue spectra. They concluded that neutron-capture elements in M15 are of pure r-process origin based upon their detailed abundance analysis. The Ba abundance variations imply that there were primordial chemical inhomogeneities in the proto-globular cluster in spite of the uniform Fe abundances.

It has been reported that there is a large scatter in the ratios of neutron-capture elements to Fe in metal-poor field stars with $[\text{Fe}/\text{H}] \leq -2.5$ (e.g., McWilliam et al. 1995; Ryan, Norris, & Beers 1996). A scatter also appears (e.g., Honda et al. 2004) in the abundance ratios between the r-process heavy elements (e.g., Ba, Eu, La) and those lighter than Ba (e.g., Y, Sr, Zr). This scatter can be interpreted (e.g., Truran et al. 2002) as a result of two processes that enrich neutron-capture elements: one generates both light and heavy r-process elements, and the other generates only light neutron-capture elements without increasing the heavy element abundances.

We have obtained high resolution blue spectra of seven red giants in M15. These data are of higher quality than that of previous studies. There are two purposes of this study: 1) to confirm the $[\text{Eu}/\text{Fe}]$ scatter in M15 stars which has been reported by Sneden et al.; and 2) to study the enrichment of other light and heavy neutron capture elements in M15. In this Letter we report the distinct result found for abundances of Y, Zr, La and Eu for six giants in M15, while the results of our full abundance analyses will be reported in a future

² $[\text{A}/\text{B}] \equiv \log(N_{\text{A}}/N_{\text{B}}) - \log(N_{\text{A}}/N_{\text{B}})_{\odot}$, and $\log \epsilon(\text{A}) \equiv \log(N_{\text{A}}/N_{\text{H}}) + 12$ for elements A and B.

publication.

2. Observations

We have selected seven red giants in M15 from the list of Sneden et al. (1997) to cover stars having high and low abundances of Ba and Eu. For comparison purposes we also observed the bright halo red giant HD 221170. This comparison star is known to have a moderate enhancement of r-process elements (Yushchenko et al. 2005).

High resolution spectroscopy was obtained with the Subaru Telescope High Dispersion Spectrograph (HDS; Noguchi et al. 2002) on July 25 and 26, 2004. The typical seeing resolution was 0.45 arcsec. This excellent seeing was very important as it allowed us to separate the target from surrounding stars in the cluster. The wavelength range covered was 3550–5250 Å, with a resolving power $R = 50,000$. Five 30 minute exposures were obtained for K146 and K1040, which are the faintest stars at the B magnitude among our sample. Three exposures (for a total of 90 minutes) were obtained for the other stars. HD 221170 was observed with the same setup. Another spectrum of this object covering 4030–6800 Å with similar quality was obtained in June 2005 to measure Ba and Eu lines in the red range.

Standard data reduction procedures (bias subtraction, flat-fielding, background subtraction, extraction, and wavelength calibration) were carried out with the IRAF echelle package³. The number of photons collected at 4300 Å for M15 stars ranges from 10,400 to 12,000 per 0.18 km s⁻¹ pixel, indicating that our data set is quite homogeneous. After the data reduction, one star (K479) was excluded from our analysis because this star shows significantly broadened spectral lines. This suggests a significant contamination from the light of other stars, even though no signature of this contamination was found in our slit viewer image nor in the archived HST image.⁴ Figure 1 shows a comparison of the spectra of K462 and K634 that have very similar features due to Fe I, Fe II, and Mn II. However, the absorption features due to neutron-capture elements are significantly stronger in K462 than in K634. Moreover, the comparison at 5123 Å (lower panel) demonstrates that the difference in the La abundance between the two stars is greater than the difference for Y.

³IRAF is distributed by the National Optical Astronomy Observatories, which is operated by the Association of Universities for Research in Astronomy, Inc. under cooperative agreement with the National Science Foundation.

⁴The images are based on observations made with the NASA/ESA Hubble Space Telescope, obtained from the data archive at the Space Telescope Science Institute. STScI is operated by the Association of Universities for Research in Astronomy, Inc. under NASA contract NAS 5-26555.

The equivalent widths of neutron-capture elements given in Table 1, and also iron, were measured by Gaussian fitting. We have applied the standard abundance analysis with SPTOOL (Y. Takeda, private communication) using model atmospheres of Kurucz (1993) to these measured equivalent widths. The spectrum synthesis technique was applied to the absorption lines of some neutron-capture elements where blending with other features or hyperfine splitting significantly affects the apparent line widths.

We adopted the effective temperatures determined by Sneden et al. (1997) in our analysis. Surface gravities (g) were determined from the ionization balance between Fe I and Fe II, while the micro-turbulence (v_{turb}) was determined from the Fe I lines by demanding that there be no dependence of the derived abundance on the equivalent widths.

We selected lines that are detected in all of the stars in our sample (Table 1) to obtain final abundances of neutron-capture elements. Since the Ba II resonance lines at 4554 and 4934 Å are very strong and inappropriate for the abundance measurements, we adopted the equivalent widths of the three lines in the red spectral range measured by Sneden et al. (1997) to determine the Ba abundances. We excluded the Eu II line at 3819 Å because of severe blending with other features. We adopted the lines at 4129 and 4205 Å measured for our spectra, and the equivalent widths of the 6645 Å line provided by Sneden et al. (1997). In the analyses of the Ba II, La II and Eu II lines, the effects of hyperfine splitting were included (see Honda et al. 2004, for more details). Though the Sr abundance is determined from the Sr II 4077 Å line, we do not include its abundance in the following discussion because an abundance deduced from only a single line is quite uncertain even though it is a strong line.

We estimated the random error from the standard deviation of the abundances determined from the individual lines for each element in each star. Since the data quality of our M15 sample is homogeneous and the abundances were determined using identical line sets, we adopted the average of these standard deviations of the six M15 stars as a measure of the random error for each element. These are given in Table 2. Systematic errors of $\lesssim 0.1$ dex due to the uncertainties of atmospheric parameters were estimated from the analyses by changing the parameters (see also Sneden et al. 1997). However, the abundance ratios of neutron-capture elements determined from species with the same ionization stage are insensitive to changes in the atmospheric parameters (Honda et al. 2004). Hence, we neglect these systematic errors when discussing abundance *ratios* between neutron-capture elements (e.g., [Y/Eu]). However, they are included when the abundances of neutron-capture elements (e.g., [Eu/H]) are discussed.

We found excellent agreement between our results for the Fe and Eu abundances and those deduced by Sneden et al. (1997) for the six M15 stars, given the solar abundances adopted in their work. The detailed abundance measurements of neutron-capture elements

were reported by Sneden et al. (2000b) for K462. We found some systematic differences (0.4 dex) in the $\log \epsilon$ values between our results and theirs, which are not explained by the small differences of atmospheric parameters adopted by the two studies. Since the line list used for their analyses is not available, we could not investigate the reason for the discrepancy. However, the differences of the abundance *ratios* of Y/Eu, Zr/Eu and La/Eu, which are discussed in the next section, are 0.01, 0.07, and 0.14 dex, respectively. We here conclude that there is no significant discrepancy in the abundance ratios between our work and previous studies by Sneden et al. We note that the quality of our spectra for the blue range is higher than those of Sneden et al. (2000b), and our study used the updated line list of La by Lawler et al. (2001a).

3. Discussion

Figure 2 shows the abundance ratios of neutron-capture elements as a function of the Eu abundance, an indicator of the enrichment by the main r-process. For comparison purposes, the values of HD 221170 and results of previous studies for r-process enhanced stars (CS 31082–001 and CS 22892–052) and the well studied star HD 122563, which has a relatively low Eu abundance, are also shown. We note that, although there are several studies for these stars (e.g., Hill et al. 2002; Sneden et al. 2003; Westin et al. 2000), we here present the results of Honda et al. (2004, 2006) who adopted the same technique and model atmosphere grid in their analysis.

There are two stars of M15 with higher abundances of neutron-capture elements of $[\text{Eu}/\text{H}] \sim -1.5$, while others have lower values of $[\text{Eu}/\text{H}] \sim -2.0$. Nevertheless, the abundance ratios of La/Eu (and Ba/Eu) are constant within the uncertainties (see the top panel of Fig. 2). These values are in good agreement with those of halo stars as well as those of the r-process component in solar-system material. These results confirm the conclusion of Sneden et al. (1997) that (1) there are star-to-star abundance variations in heavy neutron-capture elements, and (2) the heavy neutron-capture elements in M15 have primarily originated from the r-process. Note that we deliberately selected stars with relatively high and low Ba abundances from the list of Sneden et al. (1997). At this point, it is still unclear as to whether the r-process elemental abundances in M15 vary in a bimodal or continuous fashion.

In contrast to the La/Eu ratio, the ratios of Y/Eu and Zr/Eu, representing the abundance ratios of light to heavy neutron-capture elements show clear anti-correlations with the Eu abundance. The difference of the averages of the $[\text{Y}/\text{Eu}]$ values for the four stars with low $[\text{Eu}/\text{H}] (\sim -2)$ and for the other two ($[\text{Eu}/\text{H}] \sim -1.5$) is 0.34 dex, which is three times larger than the measurement error of the Y/Eu ratio. (The differences of the averages of $[\text{Zr}/\text{Eu}]$

values is 0.26 dex, which is only 1.5 times of the measurement error.) The abundance ratios produced by the main r-process are estimated from the values of the r-process enhanced halo stars. The ratios in M15 stars show excesses of the light neutron-capture elements with respect to the values found in r-process enriched field stars, and the excesses are larger in stars with lower Eu abundances.

As in the context of field halo stars (e.g. Aoki et al. 2005), an excess of light neutron capture elements can be explained by assuming two sources of neutron-capture elements: one provided light neutron-capture elements, and the other produced both light and heavy ones (the so-called main r-process). An example of field halo stars representing the result of the former process is HD 122563, whose abundance ratios are shown in Figure 2. The characteristics of this process have been studied in previous works (e.g., Truran et al. 2002; Travaglio et al. 2004), though the mechanism and the site are not yet identified. Our results indicate that such a source of light neutron-capture elements operated in M15 or its progenitor. This source enriched the light neutron-capture elements in the progenitor cloud of M15 almost uniformly. Subsequently, both light and heavy elements formed that were insufficiently mixed in the progenitor proto-cluster environment.

There are two possibilities which explain our results. If we assumed a simple correlation between time and the degree of mixing, this scatter can be realized if light neutron capture elements enriched the progenitor of M15 earlier than the heavier elements which were not mixed completely before star formation. Although the existence of (at least) two sources of neutron-capture elements was suggested by previous studies of field halo stars as mentioned above, no clear constraint on the time scales of the two processes has been given (Aoki et al. 2005). Our result that heavy neutron-capture elements show a larger scatter in their abundances than light ones in M15 suggests that the enrichment of light neutron-capture elements occurred in advance of the pollution of heavy ones. This implies that the astrophysical origin of the light neutron capture elements is related to more massive stars than the progenitors of the heavy r-process elements because heavier stars have a shorter lifetime. Alternatively, our results could also be explained if heavy r-process elements are dispersed less than light ones, for example, if heavy r-process elements were concentrated in a jet.

In either case, the dynamics of mixing of supernova ejecta and the ISM plays a critical role. Unfortunately, we know little about mixing in the early Galaxy. Our results suggest that the dynamics of mixing is non-negligible even in globular-cluster progenitor clouds, although it is usually neglected on this scale in current galactic chemical evolution models. Few measurements of light neutron-capture elements in globular clusters have been reported to date. It would be worthwhile to study the uniformity of the r-process abundance distribution

in other metal-poor globular clusters to clarify the onset of mixing in the proto-cluster environment.

This work is supported at the University of Chicago in part by the National Science foundation under Grant PHY 02-16783 for the Physics Frontier center “ Joint Institute for Nuclear Astrophysics(JINA)”. Work at the University of Notre Dame was supported by the U.S. Department of Energy under Nuclear Theory Grant DE-FG02-95-ER40934.

REFERENCES

- Aoki, W. et al. 2005, ApJ, 632, 611
- Asplund, M., Grevesse, N., & Sauval, A. J. 2005, ASP conf. series, 336, 25, astro-ph/0410214
- Hill, V. et al. 2002, A&A, 387, 560
- Honda, S., Aoki, W., Kajino, T., Ando, H., Beers, T. C., Izumiura, H., Sadakane, K., & Takada-Hidai, M. 2004, ApJ, 607, 474
- Honda, S., Aoki, W., Ishimaru, Y., Wanajo, S., & Ryan, S.G. 2006, ApJ, in press (astro-ph/0602107)
- Johnson, J. A. & Bolte, M. 2004, ApJ, 605, 462
- Kurucz, R. L., 1993, CD-ROM 13, ATLAS9 Stellar Atmospheres Programs and 2 km/s Grid (Cambridge: Smithsonian Astrophys. Obs.)
- Lawler, J. E., Bonvallet, G., & Sneden, C. 2001, ApJ, 556, 452
- Lawler, J.E., Wickliffe, M.E., Den Hartog, E.A., & Sneden, C., 2001b, ApJ, 563,1075
- McWilliam, A., Preston, G.W., Sneden, C. & Shectman, S. 1995 AJ, 109, 2736
- McWilliam, A. 1998, AJ, 115, 1640
- Noguchi, K. et al. 2002, PASJ, 54, 855
- Ryan, S.G., Norris, J.E., & Beers, T.C. 1996. ApJ, 471,254
- Rutten, R.J. 1978, Sol.Phys., 56, 237
- Sneden, C., Kraft, R. P., Shetrone, M. D., Smith, G. H., Langer, G. E., & Prosser, C. F. 1997, AJ, 114, 1964

- Sneden, C., Pilachowski, C.A. & Kraft R.P. 2000a, AJ120, 1351
- Sneden, C., Johnson, J., Kraft, R. P., Smith, G. H., Cowan, J. J., & Bolte, M. S. 2000b, ApJ, 536, L85
- Sneden, C. et al. 2003, ApJ, 591, 936
- Simmerer, J., Sneden, C., Cowan, J. J., Collier, J., Woolf, V. M., Lawler, J. E. 2004, ApJ, 617, 1091
- Travaglio, C., Gallino, R. Arnone, E., Cowan, J., Jordan, F., & Sneden, C. 2004, ApJ, 601, 864
- Truran, J. W., Cowan, J. J., Pilachowski, C. A., & Sneden, C. 2002, PASP, 114, 1293
- Westin, J., Sneden, C., Gustafsson, B., & Cowan, J.J. 2000, ApJ, 530, 783
- Yushchenko, A., Gopka, V., Goriely, S., Musaev, F., Shavrina, A., Kim, C., Kang, Y. W., Kuznietsova, J., & Yushchenko, V. 2005, A&A, 430, 255

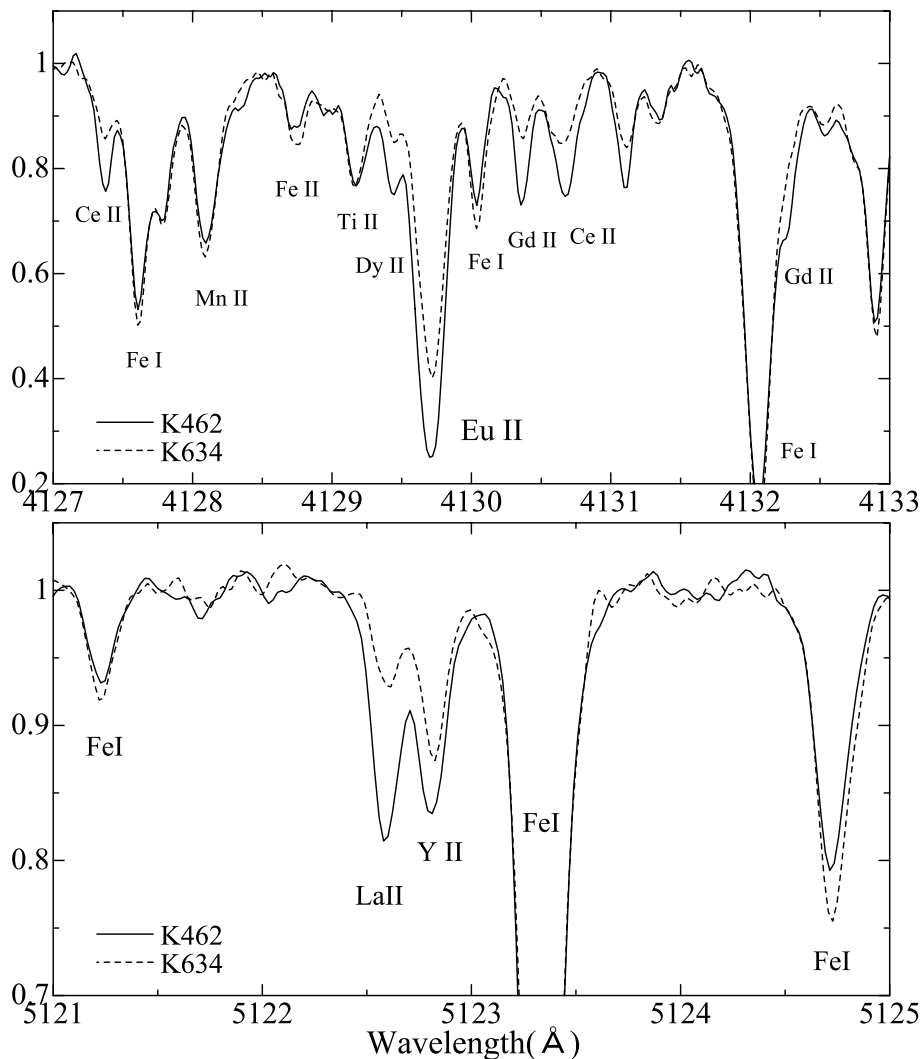


Fig. 1.— Examples of spectra of M15 stars. The upper panel shows that the absorption features of heavy neutron-capture elements (Ce, Eu, Gd, and Dy) in K462 are significantly stronger than those in K634, while the features of Ti, Fe, and Mn are almost identical. The lower panel demonstrates that the difference between the two stars of the absorption feature of the light neutron-capture element Y is not as large as that of the heavy neutron-capture element La.

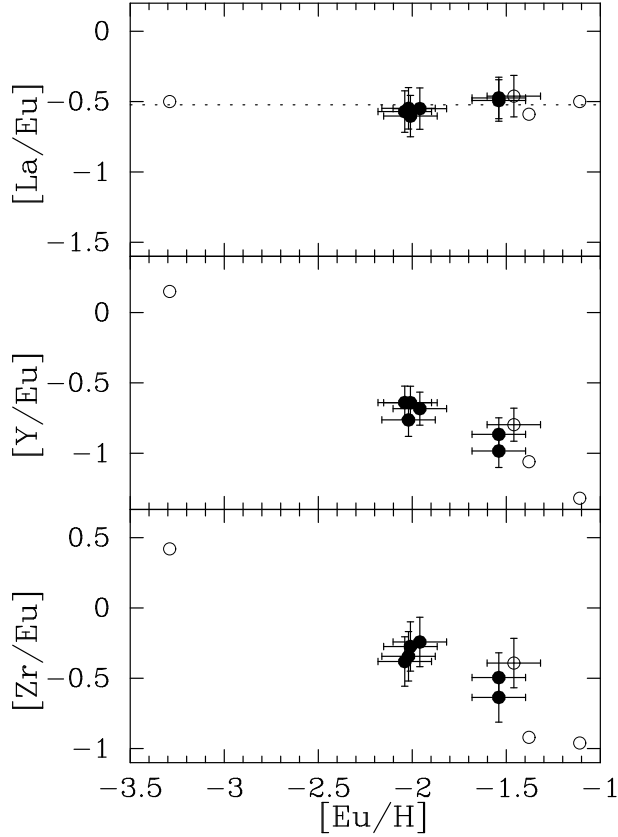


Fig. 2.— Abundance ratios between neutron-capture elements as a function of the Eu abundance ($[Eu/H]$). Filled circles are the values for M15 stars obtained in the present work, while the open circles indicate abundances of field halo stars (A symbol with error bars indicates our results for HD221170, while the other three are from Honda et al. 2004; the star with a low Eu abundance is HD 122563, and the others are the r-process enhanced stars CS 31082–001 and CS 22892–052). The dotted line drawn on the top panel is the La/Eu ratio of the solar-system r-process component (Simmerer et al. 2004).

Table 1. EQUIVALENT WIDTHS OF LINES OF NEUTRON-CAPTURE ELEMENTS

Species	Wavelength (Å)	χ (eV)	$\log gf$	equivalent widths (mÅ) ^a						
				K146	K386	K462	K490	K634	K1040	HD221170
Sr II	4077.72	0.000	0.150	175.7*	252.6*	220.6*	175.1*	204.3*	198.3*	277.2*
Y II	4854.87	0.990	−0.380	26.0	40.7	50.8	30.9	38.6	43.2	45.5
Y II	4883.68	1.080	0.070	44.7	55.4	72.1	47.3	58.7	55.1	65.2
Y II	5087.42	1.080	−0.170	29.8	44.4	55.5	33.3	44.3	44.8	48.5
Y II	5123.21	0.990	−0.830	11.0*	19.8*	26.1*	14.9*	20.5*	21.6*	24.3*
Y II	5200.41	0.990	−0.570	20.2	33.0	47.2	23.7	32.9	35.1	39.1
Zr II	3998.97	0.560	−0.670	55.1	64.4*	64.5*	33.9*	52.9*	57.6*	64.3
Zr II	4050.33	0.710	−1.000	19.7	37.3	40.6	21.1	30.1	32.1	37.1
Zr II	4161.21	0.710	−0.720	50.0	56.9*	66.6*	38.2*	52.9*	61.4*	58.4*
Zr II	4208.98	0.710	−0.460	53.1	71.4	77.5	47.4	69.9	70.3	70.7
Zr II	4317.30	0.710	−1.380	12.6	20.8	34.4	22.4	29.0	25.9	25.5
Ba II ^b	4554.03	0.000	0.170	179.3	223.0	240.4	169.9	203.6	211.9	198.0
Ba II ^b	4934.10	0.000	−0.150	180.9	223.7	235.8	177.1	206.8	212.7	208.1
Ba II ^c	5853.69	0.604	−1.010	61.0	80.0	94.0	60.0	76.0	89.0	90.7
Ba II ^c	6141.73	0.704	−0.070	112.0	133.0	145.0	108.0	120.0	143.0	137.0
Ba II ^c	6496.91	0.604	−0.380	110.0	129.0	148.0	113.0	133.0	139.0	137.4
La II	3988.52	0.400	0.210	35.5*	67.1*	94.4*	37.5*	52.3*	80.1*	83.3*
La II	3995.75	0.170	−0.060	33.0*	53.4*	79.8*	34.6*	49.6*	66.6*	72.3*
La II	4086.71	0.000	−0.070	44.8*	58.9*	87.9*	40.1*	50.8*	71.0*	64.5*
La II	4123.23	0.320	0.130	36.2*	46.9*	76.8*	34.4*	43.1*	64.4*	54.3*
La II	4333.76	0.170	−0.060	48.6*	63.1*	93.0*	51.5*	59.4*	81.9*	85.8*
La II	5123.01	0.320	−0.850	9.5*	16.4*	31.4*	12.0*	12.5*	22.0*	23.3*
Eu II ^b	3819.67	0.000	0.510	122.0*	137.6*	169.8*	90.6*	134.4*	159.0*	177.5*
Eu II	4129.70	0.000	0.220	101.9*	137.7*	178.5*	104.7*	124.7*	148.3*	156.0*
Eu II	4205.05	0.000	0.210	114.0*	166.2*	224.7*	104.5*	154.1*	193.8*	201.0*
Eu II ^c	6645.13	1.380	0.120	5.0	12.0	25.0	8.0	10.0	13.0	15.6

^aAsterisks indicate synthesized values calculated for the abundance derived by spectrum synthesis.

^bLines that were not used to derive final results.

^cEquivalent widths of M 15 stars are adopted from Sneden et al. (1997).

^dREFERENCES.– 1. Honda et al. 2004; 2. Johnson & Bolte 2004; 3. Hill et al. 2002; 4. Sneden et al. 5. McWilliam 1998; 6. Lawler et al. 2001a; 7. Lawler et al. 2001b; 8. Rutten 1978

Table 2. ATMOSPHERIC PARAMETERS AND DEDUCED CHEMICAL ABUNDANCES

Species	n	σ	$\log \epsilon(X)$							
			Sun ^a	K146	K386	K462	K490	K634	K1040	HD221170
T_{eff} (K)				4450	4200	4225	4350	4225	4450	4475
$\log g$				1.25	0.35	0.50	1.00	0.60	1.20	1.00
v_{turb}				2.00	2.25	2.25	2.05	2.05	2.40	1.70
Fe (Fe I)	54–81	0.133	7.45	5.12	5.05	5.10	5.09	5.20	5.15	5.41
Fe (Fe II)	9–13	0.148	7.45	5.11	5.04	5.11	5.09	5.21	5.15	5.41
Sr	1		2.92	0.11	0.20	0.16	−0.14	0.09	0.26	0.55
Y	5	0.041	2.21	−0.43	−0.57	−0.31	−0.47	−0.44	−0.20	−0.06
Zr	5	0.137	2.59	0.39	0.23	0.41	0.17	0.31	0.56	0.74
Ba	3	0.060	2.17	−0.34	−0.60	−0.31	−0.53	−0.45	−0.11	0.33
La	6	0.098	1.13	−1.25	−1.43	−0.96	−1.38	−1.41	−0.84	−0.79
Eu	3	0.110	0.52	−1.44	−1.50	−1.02	−1.52	−1.49	−1.02	−0.94

^aThe solar abundances taken from Asplund et al. (2005)